

# Structural and Spectroscopic Characterization of Ditungsten Halide Compounds

Kathryn M. Carlson-Day and Judith L. Eglin\*

Department of Chemistry, Mississippi State University, Mississippi State, Mississippi 39762

Chun Lin and Tong Ren

Department of Chemistry, Florida Institute of Technology, Melbourne, Florida 32901

Edward J. Valente

Department of Chemistry, Mississippi College, Clinton, Mississippi 39058

Jeffrey D. Zubkowski

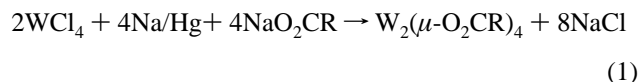
Department of Chemistry, Jackson State University, Jackson, Mississippi 39217

Received December 19, 1995<sup>⊗</sup>

The compound  $W_2(\mu-H)(\mu-O_2CC_6H_5)Br_4(\mu-dppm)_2 \cdot 2THF$  (**1**) was synthesized from  $W_2(\mu-O_2CC_6H_5)_4$ , dppm [bis(diphenylphosphino)methane], and  $Me_3SiBr$ . The analogous reaction performed using  $Me_3SiI$  resulted in the synthesis of  $W_2(\mu-O_2CC_6H_5)_2I_2(\mu-dppm)_2 \cdot solvent$  (**2**). The structures of both **1** and **2** were determined by X-ray crystallography and the following data were obtained: **1**, monoclinic  $P2_1/c$ , No. 14, with  $a = 19.173(18)$  Å,  $b = 15.104(9)$  Å,  $c = 24.049(14)$  Å,  $\beta = 111.52(6)^\circ$ ,  $V = 6479(8)$  Å<sup>3</sup>,  $Z = 4$ ,  $R1 = 0.0776$ , and  $wR^2 = 0.1333$ ; **2**, monoclinic  $C2/m$ , No. 12, with  $a = 16.969(4)$  Å,  $b = 19.189(4)$  Å,  $c = 12.195(4)$  Å,  $\beta = 127.28(2)^\circ$ ,  $V = 3159.6(14)$  Å<sup>3</sup>,  $Z = 2$ ,  $R1 = 0.0326$ , and  $wR^2 = 0.0657$ . Additional characterizations of both compounds were performed with <sup>31</sup>P NMR, <sup>1</sup>H NMR, UV–vis, and IR spectroscopy. Compound **2** and the other halide analogs can also be synthesized when  $ZnX_2$  ( $X = Cl, Br, \text{ and } I$ ) is used in the place of the silanes. The chloride and bromide analogs were characterized by <sup>31</sup>P NMR and UV–vis spectroscopy.

## Introduction

The first preparative method for ditungsten carboxylates was based loosely on the work of Schrock.<sup>1</sup> As shown in eq 1,  $WCl_4$



is reduced by sodium amalgam and the salt of the carboxylic acid is added as the ligand.<sup>2</sup> The expansion of this work has led to the synthesis of several new compounds of the general type  $W_2(\mu-O_2CR)_4$  where  $R = C_6H_5$ ,<sup>3</sup>  $CF_3$ ,<sup>2,4</sup>  $CH_3$ ,<sup>4,5</sup>  $CH_2CH_3$ ,<sup>4</sup>  $Bu$ ,<sup>4,5</sup>  $C_6H_4-p-OCH_3$ ,<sup>3</sup>  $C_6H_2[2,4,6-(CH_3)_3]$ ,<sup>3</sup> and  $C_6H_4-p-CN$ .<sup>3</sup> An alternate method that uses a dinuclear starting material is the reaction of  $1,2-W_2Et_2(NMe_2)_4$  with the acid anhydride,  $(RCO)_2O$ , where  $R = CH_3$ ,  $C_2H_5$ , and  $C(CH_3)_3$ , to form the quadruply-bonded ditungsten carboxylates.<sup>4</sup> Developed by Chisholm, this approach has been extended to the formation of ordered assemblies to form stiff-chain polymers by covalently linking the quadruply-bonded carboxylates of ditungsten and dimolybdenum.<sup>6</sup>

One of the difficulties in the study of  $W_2(\mu-O_2CR)_4$  and related compounds is their susceptibility to oxidative addition.<sup>7</sup> Developing a simpler synthetic route to multiply bonded ditungsten complexes will greatly increase the ability to vary the neutral ligands and halides in the study of the reactivity and spectroscopy of this class of compounds. Recently, a new synthetic method for  $W_2Cl_4(PR_3)_4$  type compounds has been published with an alternative reducing agent,  $NaBEt_3H$ .<sup>8</sup> This work has been extended to the synthesis of ditungsten carboxylates, specifically  $W_2(\mu-O_2CC_6H_5)_4$ .<sup>9</sup> With the simplified preparation of the starting materials, the chemistry of these carboxylates can now be readily pursued. Initial studies in this laboratory using  $W_2(\mu-O_2CC_6H_5)_4$  as a starting material with dppm and a variety of halide sources have led to complexes containing tungsten–halide bonds. We report the synthesis and spectroscopic data for several of these compounds.

## Experimental Section

**General Procedures.** Standard Schlenk, vacuum line, and drybox techniques were used with an argon atmosphere. Commercial grade tetrahydrofuran (THF), toluene, and hexanes were dried over potassium/sodium benzophenone ketyl and freshly distilled under an atmosphere of nitrogen or argon prior to use. The starting material  $WCl_4$  was synthesized from  $WCl_6$  and  $W(CO)_6$  using the previously reported method.<sup>10</sup> The dinuclear starting material  $W_2(\mu-O_2CC_6H_5)_4$  was

<sup>⊗</sup> Abstract published in *Advance ACS Abstracts*, July 1, 1996.

(1) Sharp, P. R.; Schrock, R. R. *J. Am. Chem. Soc.* **1980**, *102*, 1430.  
 (2) Sattelberger, A. P.; McLaughlin, K. W.; Huffman, J. C. *J. Am. Chem. Soc.* **1981**, *103*, 2880.  
 (3) Cotton, F. A.; Wang, W. *Inorg. Chem.* **1984**, *23*, 1604.  
 (4) Chisholm, M. H.; Chiu, H. T.; Huffman, J. C. *Polyhedron* **1984**, *3*, 759.  
 (5) Santure, D. J.; Sattelberger, A. P. *Inorg. Synth.* **1989**, *26*, 219.  
 (6) Cayton, R. H.; Chisholm, M. H.; Huffman, J. C.; Lobkovsky, E. B. *J. Am. Chem. Soc.* **1991**, *113*, 8709.

(7) Fanwick, P. E.; Harwood, W. S.; Walton, R. A. *Inorg. Chem.* **1987**, *26*, 242.

(8) Cotton, F. A.; Eglin, J. L.; James, C. A. *Inorg. Chem.* **1993**, *32*, 681.

(9) Carlson-Day, K. M.; Eglin, J. L.; Valente, E. J.; Zubkowski, J. D. *Inorg. Chim. Acta* **1996**, *244*, 151.

prepared as previously described.<sup>9</sup> The chelating phosphine dpmm was purchased from Strem Chemicals and kept under dynamic vacuum overnight to remove any residual oxygen or moisture. NaBEt<sub>3</sub>H was purchased as a 1 M solution in toluene from Aldrich and used without further purification. Me<sub>3</sub>SiBr and Me<sub>3</sub>SiI were purchased from TCI as pure liquids, transferred under argon and used without further purification. ZnCl<sub>2</sub>, ZnBr<sub>2</sub>, and ZnI<sub>2</sub> were purchased from Aldrich and placed directly into the drybox, and all subsequent transfers were performed under an argon atmosphere. <sup>31</sup>P{<sup>1</sup>H} NMR spectra (162 MHz) were recorded on a General Electric instrument using an Omega NMR spectrometer with a 10 mm broad band probe. <sup>1</sup>H NMR spectra (400 MHz) were recorded on the same spectrometer with a 5 mm probe. The UV-vis spectra were recorded on a Hewlett-Packard Model 8452 diode array spectrophotometer from 190 to 820 nm. Infrared spectra were recorded on a Midac Corporation Spectrometer Model 101280-1 with 1 cm<sup>-1</sup> resolution.

**Computational Procedure.** Molecular orbital calculations<sup>11</sup> were carried out to assess the influence of axial iodide ligands on the quadruply-bonded ditungsten compound W<sub>2</sub>(μ-O<sub>2</sub>CC<sub>6</sub>H<sub>5</sub>)<sub>2</sub>I<sub>2</sub>(μ-dppm)<sub>2</sub>. The simplifications to the system include the replacement of benzoate with formate and the chelating phosphine dpmm with two PH<sub>3</sub> groups where the P-H bond distance is 1.419 Å and the H-P-H bond angle is 93.6°, which led to the model compound W<sub>2</sub>(μ-O<sub>2</sub>CH)<sub>2</sub>I<sub>2</sub>(PH<sub>3</sub>)<sub>4</sub>. The geometrical parameters for the first coordination sphere of the W<sub>2</sub> core, including both iodides, were taken from X-ray data and averaged to yield a D<sub>2h</sub> point symmetry for the model compound. The master coordinates were chosen so the Z axis parallels the W-W vector and the XZ plane contains both formate ligands while the YZ plane contains all the P atoms. The calculations were performed on a VAXstation 4000 VLC.

**Preparation of W<sub>2</sub>(μ-H)(μ-O<sub>2</sub>CC<sub>6</sub>H<sub>5</sub>)Br<sub>4</sub>(μ-dppm)<sub>2</sub>·2THF (1).** A toluene solution of 0.20 g of W<sub>2</sub>(μ-O<sub>2</sub>CC<sub>6</sub>H<sub>5</sub>)<sub>4</sub> (0.23 mmol), 0.25 g dpmm (0.65 mmol), and 0.25 mL Me<sub>3</sub>SiBr (1.89 mmol) was gently heated and stirred for 1 h. A brown precipitate with green casts was obtained. After all solvent was removed, the green-brown product was dissolved in 4 mL of THF and precipitated from solution with 30 mL of hexanes and the solvent removed from the solid precipitate. The crude product was washed several times with 20 mL aliquots of hexanes. After the product was dried under vacuum, the solid was dissolved in THF and filtered through Celite. The final product was precipitated with 30 mL of hexanes and washed with 20 mL aliquots of hexanes and all solvent removed under vacuum to yield a green-brown solid (0.19 g, 51%). Visible spectrum (THF, λ<sub>max</sub>, nm): 428 sh. IR (KBr pellet, CO stretches, cm<sup>-1</sup>): 1435 s, 1411 s.

**Preparation of W<sub>2</sub>(μ-O<sub>2</sub>CC<sub>6</sub>H<sub>5</sub>)<sub>2</sub>I<sub>2</sub>(μ-dppm)<sub>2</sub>·solvent (2). Method A.** A mixture of 1.00 g of WCl<sub>4</sub> (3.07 mmol) and 0.82 g Na(O<sub>2</sub>CC<sub>6</sub>H<sub>5</sub>) (5.69 mmol) was suspended in 20 mL of THF. After the flask was cooled to -60 °C and 6.14 mL of NaBEt<sub>3</sub>H (6.14 mmol) added, the reaction was allowed to warm to room temperature. Once the reaction mixture had changed color from the initial gray to a brilliant purple indicating formation of W<sub>2</sub>(μ-O<sub>2</sub>CC<sub>6</sub>H<sub>5</sub>)<sub>4</sub>, 1.08 g of dpmm (2.81 mmol) and 1.07 mL of Me<sub>3</sub>SiI (7.52 mmol) were added. The reaction mixture was gently heated for 24 h, resulting in a reddish-orange solution with a red precipitate. Hexanes (30 mL) were added to the solution and the precipitate washed several times with 10-20 mL aliquots of hexanes. After solvent removal, a red solid (2.36 g, 94.0%) was obtained. Visible spectrum (THF, λ<sub>max</sub>, nm): 400 sh. IR (KBr pellet, CO stretches, cm<sup>-1</sup>): 1433 s, 1409 s.

**Method B.** A mixture of 0.20 g of WCl<sub>4</sub> (0.61 mmol) and 0.16 g of Na(O<sub>2</sub>CC<sub>6</sub>H<sub>5</sub>) (1.11 mmol) was suspended in 10 mL of THF. After the solution was cooled to -70 °C, 1.23 mL of NaBEt<sub>3</sub>H (1.23 mmol) was added and the reaction allowed to warm to room temperature to yield the intermediate, W<sub>2</sub>(μ-O<sub>2</sub>CC<sub>6</sub>H<sub>5</sub>)<sub>4</sub>. To this crude product, a THF solution of 0.22 g of dpmm (0.57 mmol) and 0.30 g of ZnI<sub>2</sub> (0.94 mmol) was added. The mixture was gently heated for 1 h, and a reddish-orange solution with a red precipitate was obtained. Several aliquots of hexanes (30 mL) were added to wash the solution, followed by solvent removal to yield the product W<sub>2</sub>(μ-O<sub>2</sub>CC<sub>6</sub>H<sub>5</sub>)<sub>2</sub>I<sub>2</sub>(μ-dppm)<sub>2</sub>·solvent (0.24 g, 48%).

**Preparation of W<sub>2</sub>(μ-O<sub>2</sub>CC<sub>6</sub>H<sub>5</sub>)<sub>2</sub>Cl<sub>2</sub>(μ-dppm)<sub>2</sub> (3).** A procedure similar to that of the iodide complex, **2**, was used in the preparation of the chloride analog. The synthetic route was analogous to that outlined in Method B except that ZnCl<sub>2</sub> (0.13 g, 0.95 mmol) was used instead of ZnI<sub>2</sub> to yield W<sub>2</sub>(μ-O<sub>2</sub>CC<sub>6</sub>H<sub>5</sub>)<sub>2</sub>Cl<sub>2</sub>(μ-dppm)<sub>2</sub> (0.39 g, 59%). The amounts of the starting material WCl<sub>4</sub> and the other reagents used were the same as in Method B. Visible spectrum (THF, λ<sub>max</sub>, nm): 454 sh.

**Preparation of W<sub>2</sub>(μ-O<sub>2</sub>CC<sub>6</sub>H<sub>5</sub>)<sub>2</sub>Br<sub>2</sub>(μ-dppm)<sub>2</sub> (4).** The bromide analog was obtained by Method B using 0.21 g of ZnBr<sub>2</sub> (0.93 mmol) instead of ZnI<sub>2</sub> to yield W<sub>2</sub>(μ-O<sub>2</sub>CC<sub>6</sub>H<sub>5</sub>)<sub>2</sub>Br<sub>2</sub>(μ-dppm)<sub>2</sub> (0.15 g, 34%). The amounts of starting material WCl<sub>4</sub> and the other reagents used were the same as in Method B. Visible spectrum (THF, λ<sub>max</sub>, nm): 438 sh.

**Crystallographic Studies.** Crystals of W<sub>2</sub>(μ-H)(μ-O<sub>2</sub>CC<sub>6</sub>H<sub>5</sub>)Br<sub>4</sub>(μ-dppm)<sub>2</sub>·2THF and W<sub>2</sub>(μ-O<sub>2</sub>CC<sub>6</sub>H<sub>5</sub>)<sub>2</sub>I<sub>2</sub>(μ-dppm)<sub>2</sub>·solvent grown from THF/hexanes solvent mixtures were mounted onto glass fibers using epoxy cement. Data for each of these samples were collected on a Siemens R3m/V automated diffractometer fitted with a molybdenum source and a graphite monochromator (wavelength = Kα = 0.710 73 Å).<sup>12</sup> Automatic peak search and indexing procedures yielded monoclinic cells for both crystals and inspection of the Niggli values revealed no conventional cell of higher symmetry.

The structure of W<sub>2</sub>(μ-H)(μ-O<sub>2</sub>CC<sub>6</sub>H<sub>5</sub>)Br<sub>4</sub>(μ-dppm)<sub>2</sub>·2THF was determined using direct methods<sup>13</sup> in space group P2<sub>1</sub>/c and refined by full-matrix least-squares methods.<sup>14</sup> The hydrogen atom positions on carbon atoms in the ligands were assigned idealized locations: the bridging hydrogen was not discernible but inferred from the geometry of the complex. The hydrogen atoms were included in structure factor calculations but only the coordinates and vibrational factors of the non-hydrogen atoms were refined. After completion of the refinement of all non-hydrogen atoms with isotropic vibrational parameters, the deviations between the stronger unweighted observed and corresponding calculated structure factors based on the model were examined in conjunction with the direction cosines for each diffraction vector. An absorption model was constructed empirically using SHELXA-90<sup>15</sup> and refined to fit the larger deviations. Before this absorption model was applied, the corrections were examined and found to be consistent with the calculated absorption coefficient and known crystal dimensions. Scattering factors were taken from ref 16. In the refinement, all data were used.

The structure of W<sub>2</sub>(μ-O<sub>2</sub>CC<sub>6</sub>H<sub>5</sub>)<sub>2</sub>I<sub>2</sub>(μ-dppm)<sub>2</sub>·solvent was found in space group C2/m using direct methods<sup>13</sup> which revealed most of the non-hydrogen atoms. The remaining atoms were determined from subsequent difference Fourier calculation maps.<sup>14</sup> Hydrogen atom positions on carbons in the ligands were assigned idealized locations. The hydrogen atom positions and isotropic vibrational factors were included in the structure factor calculations, but were not refined. An empirical absorption correction<sup>17</sup> appeared to be necessary and was determined and applied to the data based on ψ scans at the end of data collection for five reflections: (0, 3, 4), (1, 3, 4), (1, 4, 5), (0, 5, 6), and (1, 5, 6).

An unidentified solvent molecule, modeled with four half-occupancy carbon atoms (C(1S), C(2S), C(3S), C(4S)), was included in the refinement with isotropic vibrational factors. Crystals of **2** were grown from tetrahydrofuran solutions layered with hexanes and the resulting 12 atom locations, representing eight carbons, are consistent with either a five- or six-atom cyclic or chain molecule. Since the model solvent is nearly planar and one atom lies on a 2-fold axis, another lies on a mirror plane, and two lie in general positions surrounding a crystallographic 2/m site, neither solvent has the correct symmetry. Only weak features remain in the vicinity of the model solvent atoms in the final difference Fourier maps and such small solvent scattering is

(10) Schrock, R. R.; Sturgeoff, L. G.; Sharp, P. R. *Inorg. Chem.* **1983**, *22*, 2801.

(11) Hall, M. B.; Fenske, R. F. *Inorg. Chem.* **1972**, *11*, 768.

(12) Diffractometer data collection controlled by P3-PC version (Siemens Analytical X-Ray Instruments, Inc. Madison, WI).

(13) Sheldrick, G. M. *Acta Crystallogr.* **1990**, *A46*, 467.

(14) Sheldrick, G. M. *Crystallographic Computing*; Oxford University Press: Oxford, U.K., 1992; pp 111-122.

(15) SHELXA-90 Version 1, Siemens Analytical X-Ray Instruments, Inc., Madison, WI.

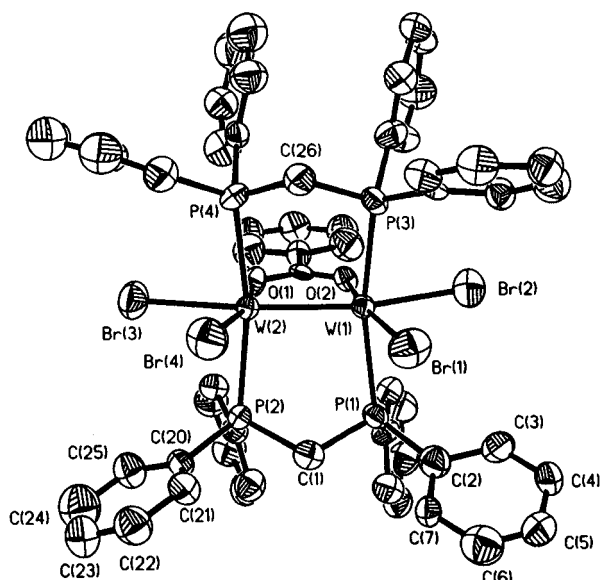
(16) *International Tables for X-Ray Crystallography*; D. Reidel Publishing: Dordrecht, The Netherlands, 1985; Vol. IV.

(17) XEMP, Siemens Industrial X-Ray, Madison WI.

**Table 1.** Crystal Data for Compounds **1** and **2**

	$W_2(\mu-H)(\mu-O_2CC_6H_5)Br_4(\mu-dppm)_2 \cdot 2THF$ ( <b>1</b> )	$W_2(\mu-O_2CC_6H_5)_2I_2(\mu-dppm)_2 \cdot \text{solvent}$ ( <b>2</b> )
formula	$C_{57}H_{50}Br_4O_2P_4W_2 \cdot 2OC_6H_8$	$C_{64}H_{54}I_2O_4P_4W_2 \cdot \frac{1}{2}OC_4H_8 \cdot \frac{1}{2}C_6H_{14}$
fw	1722.48	1711.70
temp, K	295(2)	295(2)
wavelength, Å	0.71073	0.71073
cryst syst	monoclinic	monoclinic
space group	$P2_1/c$ (No. 14)	$C2/c$ (No. 12)
<i>a</i> , Å	19.173(18)	16.969(4)
<i>b</i> , Å	15.104(9)	19.189(4)
<i>c</i> , Å	24.049(14)	12.195(4)
$\beta$ , deg	111.52(6)	127.28(2)
<i>V</i> , Å <sup>3</sup>	6479(8)	3159.6(14)
<i>Z</i>	4	2
<i>d</i> <sub>calc</sub> , Mg/m <sup>3</sup>	1.766	1.799
abs coeff, mm <sup>-1</sup>	6.16	4.840
cryst size, mm	0.25 × 0.20 × 0.20	0.15 × 0.08 × 0.06
$\theta$ range for data collcn, deg	1.76 to 20.02	1.84 to 32.50
index ranges	$0 \leq h \leq 18, 0 \leq k \leq 14, -19 \leq l \leq 21$	$-23 < h < 20, -26 < k < 28, 0 < l < 17$
no. of reflns collcd	6084	10463
no. of indep reflns	5864 [ <i>R</i> (int) = 0.0807]	5463 [ <i>R</i> (int) = 0.0452]
refinement method	full-matrix least-squares on <i>F</i> <sup>2</sup>	full-matrix least-squares on <i>F</i> <sup>2</sup>
data/restraints/params	5864/348/669	5463/0/193
<i>R</i> <sup>a</sup>	0.0776	0.0326
<i>R</i> <sub>w</sub> <sup>b</sup>	0.1333 <sup>c</sup>	0.0657 <sup>d</sup>

<sup>a</sup>  $R = \sum ||F_o| - |F_c|| / \sum |F_o|$ . <sup>b</sup>  $R_w = [\sum (wF_o^2 - F_c^2)^2 / \sum (wF_o^4)]^{1/2}$ . <sup>c</sup> weight =  $1/\sigma^2(F_o^2) + (0.0383P)^2 + 144.75P$ , where  $P = (\max(F_o^2, 0) + 2F_c^2)/3$ . <sup>d</sup> weight =  $1/\sigma^2(F_o^2) + (0.02780P)^2 + 0P$ , where  $P = (\max(F_o^2, 0) + 2F_c^2)/3$ .

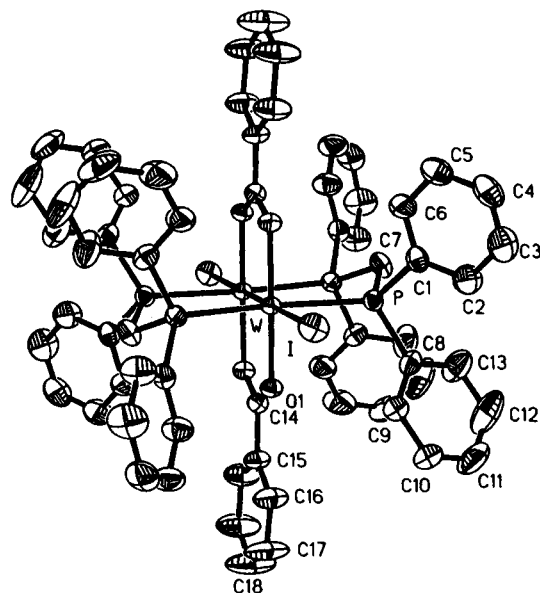
**Figure 1.** 50% probability thermal ellipsoid plot of  $W_2(\mu-H)(\mu-O_2CC_6H_5)Br_4(\mu-dppm)_2$  viewed perpendicular to the W–W axis.

unlikely to affect the modeling and interpretation of the more electron-rich ditungsten complex. Since spectroscopic methods have eliminated the possibility that  $W_2(\mu-O_2CC_6H_5)_2I_2(\mu-dppm)_2$  is ionic, the unidentified solvent molecule is neither a cation or an anion. The density and formula weight calculations provided in Table 1 are based on one molecule of solvent for each  $W_2(\mu-O_2CC_6H_5)_2I_2(\mu-dppm)_2 \cdot \text{solvent}$  with site occupancy of 0.50 THF and 0.50 hexanes. The final difference features did not exceed  $+1.913 \text{ e } \text{Å}^{-3}$  and  $-1.670 \text{ e } \text{Å}^{-3}$  with the greater positive features near W and I. Scattering factors were taken from ref 16.

The structures of  $W_2(\mu-H)(\mu-O_2CC_6H_5)Br_4(\mu-dppm)_2 \cdot 2THF$  and  $W_2(\mu-O_2CC_6H_5)_2I_2(\mu-dppm)_2 \cdot \text{solvent}$  are shown in Figures 1 and 2 respectively. Pertinent crystallographic parameters for **1** and **2** are summarized in Table 1. Selected bond lengths and angles for **1** and **2** are listed in Tables 2 and 3.

## Results and Discussion

**Preparation and General Properties.** The preparation of  $W_2(\mu-H)(\mu-O_2CC_6H_5)Br_4(\mu-dppm)_2 \cdot 2THF$  was analogous to that

**Figure 2.** Thermal ellipsoid plot of  $W_2(\mu-O_2CC_6H_5)_2I_2(\mu-dppm)_2$  viewed at approximately 45° to the W–W axis. Thermal ellipsoids for W, I, P, O, and C atoms are shown at 50% probability.

of the chloro complex  $W_2(\mu-H)(\mu-O_2CC_6H_5)Cl_4(\mu-dppm)_2$ .<sup>9</sup> The use of the  $W_2(\mu-O_2CC_6H_5)_4$  as the starting material, made *in situ*, enables the facile preparation and avoids the isolation and transfer of this highly sensitive starting material. Not only can  $W_2(\mu-O_2CC_6H_5)_4$  be used without further purification *in situ*, but this starting material is more stable than the trifluoroacetate analog.<sup>18</sup> While this added stability makes  $W_2(\mu-O_2CC_6H_5)_4$  somewhat easier to handle, to date only a maximum of three of the benzoate ligands have been substituted instead of the four necessary to produce the desired products  $W_2X_4(\mu-dppm)_2$ .<sup>19–23</sup>

(18) Santure, D. J.; McLaughlin, K. W.; Huffman, J. C.; Sattelberger, A. P. *Inorg. Chem.* **1983**, *22*, 1877.

(19) Cotton, F. A.; Falvello, L. R.; Harwood, W.; Powell, G. L.; Walton, R. A. *Inorg. Chem.* **1986**, *25*, 3949.

(20) Cotton, F. A.; Dunbar, K. R.; Poli, R. *Inorg. Chem.* **1986**, *25*, 3700.

(21) Chen, J. D.; Cotton, F. A.; Falvello, L. R. *J. Am. Chem. Soc.* **1990**, *112*, 1076.

**Table 2.** Selected Bond Distances (Å) and Angles (deg) for  $W_2(\mu-H)(\mu-O_2CC_6H_5)Br_4(\mu-dppm)_2 \cdot 2THF$ 

Distances			
W(1)–W(2)	2.535(2)	W(1)–P(3)	2.550(9)
W(1)–Br(1)	2.529(4)	W(2)–P(4)	2.548(8)
W(1)–Br(2)	2.655(4)	W(2)–O(1)	2.07(2)
W(2)–Br(3)	2.677(4)	W(1)–O(2)	2.08(2)
W(2)–Br(4)	2.518(4)	O(1)–C(51)	1.23(3)
W(1)–P(1)	2.565(8)	O(2)–C(51)	1.13(3)
W(2)–P(2)	2.565(8)		
Angles			
Br(1)–W(1)–W(2)	109.79(11)	O(1)–W(2)–P(4)	93.8(6)
W(2)–W(1)–Br(2)	157.96(10)	Br(1)–W(1)–P(1)	81.4(2)
W(1)–W(2)–Br(3)	162.63(10)	Br(4)–W(2)–P(2)	88.1(2)
Br(4)–W(2)–W(1)	109.30(11)	Br(1)–W(1)–P(3)	82.4(2)
W(2)–W(1)–P(1)	96.2(2)	Br(4)–W(2)–P(4)	83.8(2)
W(1)–W(2)–P(2)	94.9(2)	P(3)–W(1)–P(1)	162.6(3)
W(2)–W(1)–P(3)	95.1(2)	P(4)–W(2)–P(2)	168.7(3)
W(1)–W(2)–P(4)	95.3(2)	Br(1)–W(1)–Br(2)	92.24(14)
O(1)–W(2)–W(1)	86.0(5)	Br(4)–W(2)–Br(3)	88.06(14)
O(2)–W(1)–W(2)	82.0(5)	P(1)–W(1)–Br(2)	87.5(2)
O(2)–W(1)–Br(1)	167.8(5)	P(2)–W(2)–Br(3)	84.9(2)
O(2)–W(1)–Br(2)	76.0(5)	P(3)–W(1)–Br(2)	87.0(2)
O(2)–W(1)–P(1)	94.5(5)	P(4)–W(2)–Br(3)	86.9(2)
O(1)–W(2)–P(2)	91.9(6)	O(1)–W(2)–Br(3)	76.6(6)
O(2)–W(1)–P(3)	100.1(5)	O(1)–W(2)–Br(4)	164.6(6)

**Table 3.** Selected Bond Distances (Å) and Angles (deg) for  $W_2(\mu-O_2CC_6H_5)_2I_2(\mu-dppm)_2 \cdot \text{solvent}^a$ 

Distances			
W–W	2.2925(6)	W–O(1)	2.083(2)
W–I	3.1033(7)	W–P	2.5572(13)
Angles			
W'–W–I	180.0	O(1)–W–P'	88.82(7)
W'–W–P	98.42(2)	O(1)'–W–P'	91.43(7)
O(1)–W–W'	89.15(6)	P–W–I	81.58(2)
O(1)'–W–W'	89.15(6)	P'–W–I	81.58(2)
O(1)–W–I	90.85(6)	P–W–P'	163.17(4)
O(1)'–W–I	90.85(6)	O(1)'–W–O(1)	178.31(2)
O(1)–W–P	91.43(7)	W'–W–P'	98.42(2)
O(1)'–W–P	88.82(7)		

<sup>a</sup> Symmetry transformations used to generate equivalent atoms: W',  $-x, -y + 1, -z$ ; P',  $x, -y + 1, z$ ; O(1)',  $-x, y, -z$ .

The presence of acid in the reaction mixture, a result of the choice of the halide source  $Me_3SiBr$ , seems to promote the loss of a third carboxylate ligand. Commercial grade silanes are not usually packed in ampules under argon with the exception of the highly reactive  $Me_3SiI$ , a key to the difference in the reactions using  $Me_3SiBr$  versus  $Me_3SiI$ . The resultant water contamination and subsequent acid production in  $Me_3SiBr$  resulted in the presence of a bridging hydride in  $W_2(\mu-H)(\mu-O_2CC_6H_5)Br_4(\mu-dppm)_2 \cdot 2THF$ . However, even though there was no acid contamination of the  $Me_3SiI$ , the product obtained,  $W_2(\mu-O_2CC_6H_5)_2I_2(\mu-dppm)_2 \cdot \text{solvent}$ , still retained two of the benzoate ligands in contrast to the analogous  $Mo_2(\mu-O_2CCH_3)_4$  and  $Mo_2(\mu-O_2CCF_3)_4$  chemistry.<sup>19–22</sup>

Our inability to substitute more than two benzoate ligands in non-acidic media for the complex  $W_2(\mu-O_2CC_6H_5)_4$  may be due to the weakly acidic carboxylic acid, benzoic acid. Benzoate ligand ( $pK_a$  of benzoic acid 4.19) is a poor leaving group relative to that of trifluoroacetate ligand ( $pK_a$  of trifluoroacetic acid 0.23), and further exchange of the benzoate ligand for halides does not occur in non-acidic media under mild reaction conditions.<sup>24</sup> The presence of an acid might be required to protonate the third

and fourth carboxylate away from the ditungsten core. If this is true, then further changes in the carboxylate groups will not change the reaction to yield the desired product,  $W_2I_4(\mu-dppm)_2$ . While carboxylate ligands have been removed easily from a dimolybdenum core, acid may drive these reactions to completion.<sup>25–28</sup> The presence of an acid in the dimolybdenum chemistry does not yield the oxidative addition products observed for the ditungsten core as shown by the preparation of  $K_4Mo_2Cl_8$  in a highly acidic reaction medium.<sup>29</sup>

The synthesis of  $W_2(\mu-O_2CC_6H_5)_2I_2(\mu-dppm)_2 \cdot \text{solvent}$  was also performed using  $ZnI_2$  as the halide source. Confirmation of the product  $W_2(\mu-O_2CC_6H_5)_2I_2(\mu-dppm)_2 \cdot \text{solvent}$  through the use of <sup>31</sup>P NMR and UV–vis spectroscopy was carried out. Since the  $ZnBr_2$  and  $ZnCl_2$  salts are commercially available, the analogous reactions were performed to yield the novel compounds  $W_2(\mu-O_2CC_6H_5)_2Cl_2(\mu-dppm)_2$  (**3**) and  $W_2(\mu-O_2CC_6H_5)_2Br_2(\mu-dppm)_2$  (**4**). While solid state structural characterization could not be performed, the presence of these complexes was confirmed via <sup>31</sup>P NMR and UV–vis spectroscopy. In contrast to the silane reagents, the absence of acid contamination in the zinc salts allowed the synthesis of  $W_2(\mu-O_2CC_6H_5)_2Cl_2(\mu-dppm)_2$  and  $W_2(\mu-O_2CC_6H_5)_2Br_2(\mu-dppm)_2$  for the first time.

**Structures.** A comparison of bond distances in  $W_2(\mu-H)(\mu-O_2CC_6H_5)Br_4(\mu-dppm)_2 \cdot 2THF$  and  $W_2(\mu-H)(\mu-O_2CC_6H_5)Cl_4(\mu-dppm)_2$  reveals almost identical  $W_2$  core structures with bond distances of 2.535(2) and 2.554(2) Å, respectively. These W–W bond distances are intermediate to those observed for the edge-sharing bioctahedral complexes  $W_2(\mu-H)(\mu-Cl)Cl_4(\mu-dppm)_2$  (2.4830(9) Å)<sup>7</sup> and  $W_2(\mu-Cl)_2Cl_4(\mu-dppm)_2$  (2.691(1) Å).<sup>30</sup>

The tungsten–halide bond distances in  $W_2(\mu-H)(\mu-O_2CC_6H_5)Br_4(\mu-dppm)_2 \cdot 2THF$  compared to those in  $W_2(\mu-H)(\mu-O_2CC_6H_5)Cl_4(\mu-dppm)_2$ <sup>9</sup> are longer due to the increase in size of the halide from Cl to Br. As in the case of  $W_2(\mu-H)(\mu-O_2CC_6H_5)Cl_4(\mu-dppm)_2$ , two types of tungsten–halide bond distances and angles are observed in  $W_2(\mu-H)(\mu-O_2CC_6H_5)Br_4(\mu-dppm)_2 \cdot 2THF$ . For the bromide atoms *trans* to the bridging hydride, the W–Br bond distances (2.677(4), 2.655(4) Å) are longer than the bond distances of the bromide atoms *trans* to the bridging benzoate, W–Br (2.518(4), 2.529(4) Å). However, this difference in the tungsten–halide bond distance is of the same order of magnitude as the one observed in the chloride analog.<sup>9</sup> In this structure, the W–W–Br bond angles reflect the distortion due to a carboxylate ligand, a three atom chain, bridging the  $W_2$  core instead of a single atom such as a halide or hydride in a typical edge-sharing bioctahedral complex. The W–W–Br angles for the bromides *trans* to the bridging benzoate (109.79(11) and 109.30(11)°) are similar to those for the quadruply-bonded compound,  $W_2Cl_4(\mu-dppm)_2$  (106.48(6) and 109.28(7)°)<sup>23</sup> while W–W–Br angles for the bromides *trans* to the bridging hydride are 157.96(10) and 162.63(10)°.

An increase in the W–W bond distance for  $W_2(\mu-O_2CC_6H_5)_2I_2(\mu-dppm)_2 \cdot \text{solvent}$  (2.2925(6) Å) is observed compared to that of the parent compound  $W_2(\mu-O_2CC_6H_5)_4$  (2.196(1) Å).<sup>3</sup> It is also longer than the W–W bond distance in the

(22) Agaskar, P. A.; Cotton, F. A.; Dunbar, K. R.; Falvello, L. R.; O'Connor, C. J. *Inorg. Chem.* **1987**, *26*, 4051.

(23) Canich, J. M.; Cotton, F. A. *Inorg. Chim. Acta* **1988**, *142*, 69.

(24) McMurry, J. *Organic Chemistry*, 2nd ed.; Brooks/Cole Publishing Company: Pacific Grove, CA, 1988; p 721.

(25) Cotton, F. A.; Walton, R. A. *Multiple Bonds Between Metal Atoms*, 2nd ed.; University Press: Oxford, U.K., 1993.

(26) Cotton, F. A.; Etxine, M. W.; Felthouse, T. R.; Kolthammer, B.; Lay, D. J. *Am. Chem. Soc.* **1981**, *103*, 4040.

(27) Cotton, F. A.; Daniels, L. M.; Powell, G. L.; Kahaian, A. J.; Smith, T. J.; Vogel, E. *Inorg. Chim. Acta* **1988**, *144*, 109.

(28) Hopkins, M.; Schaefer, W.; Bronikowski, M.; Woodruff, W.; Miszkowski, V.; Dallinger, R.; Gray, H. B. *J. Am. Chem. Soc.* **1987**, *109*, 408.

(29) Brencic, J. V.; Cotton, F. A. *Inorg. Chem.* **1970**, *9*, 351.

(30) King, M. A. S.; McCarley, R. E. *Inorg. Chem.* **1973**, *12*, 1972.

carboxylate complex containing axially coordinated phosphines,  $W_2(\mu-O_2CCF_3)_4 \cdot 2PPh_3$ .<sup>18</sup> Not only is the W–W bond in this compound longer than those found in other quadruply-bonded carboxylate compounds, but also it is one of the longest bond distances for a W(II,II) compound with a chelating phosphine.<sup>31,32</sup> This bond distance is noteworthy since the coordination geometry about the ditungsten core is essentially eclipsed without weakening of the  $\delta$  bond due to incomplete overlap.<sup>25</sup> However, the MO calculations demonstrate that the axial ligands effectively reduce the strength of the W–W  $\sigma$  bond.

In comparison to W(III,III) compounds of the general type  $W_2R_2(\mu-O_2CX)_4$ , where R is an alkyl lacking  $\beta$  hydrogens and X is an alkyl, aryl, or  $NR_2$ ,<sup>33</sup>  $W_2(\mu-O_2CC_6H_5)_2I_2(\mu-dppm)_2 \cdot$  solvent has a significantly longer W–W bond distance. If one compares the W–W–X bond angles, where X is the axially coordinated ligand, for  $W_2(\mu-O_2CC_6H_5)_2I_2(\mu-dppm)_2 \cdot$  solvent and the triply bonded Chisholm complexes,<sup>34</sup> the iodide complex is perfectly linear by symmetry, W–W–I = 180° while the angle in, for example,  $W_2(np)_2(\mu-O_2CC_6H_5)_4$  is 175.15 (11)°. This linear coordination of axial halides makes  $W_2(\mu-O_2CC_6H_5)_2I_2(\mu-dppm)_2 \cdot$  solvent a potential candidate for tying extended chains of dinuclear tungsten centers together.

The W–I bond distance for  $W_2(\mu-O_2CC_6H_5)_2I_2(\mu-dppm)_2 \cdot$  solvent in comparison to other tungsten complexes<sup>35</sup> is one of the longest, indicating weak axial coordination. This distance is 0.38 Å longer than the distance for equatorial W–I bonds (2.725 Å) expected based on the analogous molybdenum chemistry.<sup>20,36</sup> The other bond distances and angles observed fall into the range expected for dinuclear tungsten complexes.<sup>3,23,31–33</sup>

**Bonding Nature of  $W_2(\mu-O_2CC_6H_5)_2I_2(\mu-dppm)_2$ .** There are 46 occupied valence molecular orbitals in the model compound  $W_2(\mu-O_2CH)_2I_2(PH_3)_4$ . Most of the low-lying molecular orbitals are the C–H, P–H, and C–O  $\sigma$ -bond orbitals, which bear no direct relevance to the W–W bonding in  $W_2(\mu-O_2CC_6H_5)_2I_2(\mu-dppm)_2 \cdot$  solvent and are omitted from the discussion. Important information about both the high energy occupied molecular orbitals and the low energy vacant molecular orbitals is summarized in Table 4. The molecular orbitals of predominant W–W bonding character are, in order of the ascending energy,  $9a_g(\sigma)$ ,  $5b_{2u}(\pi_{yz})$ ,  $6b_{3u}(\pi_{xz})$ ,  $3b_{1g}(\delta)$ ,  $3a_u(\delta^*$ , LUMO),  $6b_{3g}(\pi_{yz}^*)$ ,  $6b_{2g}(\pi_{xz}^*)$ , and  $9b_{1u}(\sigma^*)$ . While the highest occupied metal-based orbital is the W–W  $\delta$  bonding orbital, the HOMOs are the I-based  $\pi$ -type lone pair orbitals, which is likely due to the low electronegativity of iodine. On the basis of both the orbital occupancy and the significant HOMO–LUMO gap (2.32 eV), it is clear that a W–W quadruple bond exists ( $\sigma^2\pi^4\delta^2$ ). Although the W–W interactions in this compound are similar to those described for other well-known quadruply-bonded ditungsten compounds,<sup>25</sup> several distinctive features of the electronic structure resulting from its unique structure are discussed here.

Although the metal-based orbitals can be clearly identified, the ligand contribution to these orbitals is significant, especially to the  $\sigma$ -bond orbitals. For instance, the contribution of I to

**Table 4.** Upper Valence Molecular Orbitals of  $W_2(\mu-O_2CH)_2I_2(PH_3)_4$

symbol	<i>E</i> (eV)	assignment	character (%)
$9b_{1u}$	0.20	W–W $\sigma^*$	W, $d_{z^2}$ (34), $p_z$ (32), s (8); I, $p_z$ (22)
$7b_{2u}$	0.08	$\sigma^*(C-O)$	
$6b_{2g}$	−1.34	W–W $\pi^*(xz)$	W $d_{xz}$ (92)
$6b_{3g}$	−1.40	W–W $\pi^*(yz)$	W $d_{yz}$ (93)
$3a_u$	−4.65	W–W $\delta^*$ , LUMO	W $d_{xy}$ (88)
$10a_g$	−6.97	I lone pair, HOMO	I, $p_z$ (79); W, $p_z$ (14)
$6a_{2u}$	−7.30	I lone pair	I, $p_y$ (97)
$7b_{3u}$	−7.33	I lone pair	I, $p_x$ (95)
$5b_{3g}$	−7.42	I lone pair	I, $p_y$ (97)
$5b_{2g}$	−7.54	I lone pair	I, $p_x$ (95)
$8b_{1u}$	−8.40	I lone pair	I, $p_z$ (76); W, $d_{z^2}$ (12), $p_z$ (5)
$3b_{1g}$	−8.55	W–W $\delta$	W, $d_{xy}$ (86)
$6b_{3u}$	−9.67	W–W $\pi(xz)$	W $d_{xz}$ (87); O $sp^2$ (8); I $p_x$ (5)
$5b_{2u}$	−11.22	W–W $\pi(yz)$	W $d_{yz}$ (91); $s^*$ (P–H) (6); I $p_y$ (3)
$9a_g$	−12.33	W–W $\sigma$	W, $d_{z^2}$ (64), s (17); I, $p_z$ (10)

$9a_g$  is about 10%, which effectively reduces the strength of the W–W  $\sigma$  bond. This is consistent with the elongation of W–W bond length observed. The iodine contribution to the W–W  $\sigma^*$  orbital is even greater, though it has no direct effect upon the molecular structure since  $9b_{1u}$  is empty. Correspondingly, there also exists extensive mixing of W orbitals into  $p_z$  lone pair orbitals of iodine ( $8b_{1u}$  and  $10a_g$ ).

Due to the low symmetry of the molecule, the W–W  $\pi$  bonding orbitals lose their degeneracy. The orbital with principle overlaps in the  $yz$  plane (containing the P atoms) is stabilized by 1.6 eV over that in the  $xz$  plane (containing the O atoms of the formate ligands). This may be understood on the basis that phosphines are weak  $\pi$  acids ( $\sigma^*$  (P–H) as the acceptor orbitals), while formates are weak  $\pi$  bases (the oxygen  $sp^2$  lone pairs as the donor orbitals). Both of these planar components also contain the contribution from iodine lone pairs, albeit nonbonding in nature.

Although the lack of structural information for both the chloride and bromide analogs prevents in-depth studies of their bonding natures, these compounds are also clearly quadruply-bonded, as evidenced by their diamagnetic <sup>31</sup>P chemical shifts which are within 1 ppm of the chemical shift observed for  $W_2(\mu-O_2CC_6H_5)_2I_2(\mu-dppm)_2 \cdot$  solvent. Since the significant iodine contribution to the W–W  $\sigma$ -bonding orbital is due to the low electronegativity of iodine, the analogous contributions should be drastically decreased for the chloride and bromide analogs, and significantly shortened W–W bond distances are expected for these compounds.

**NMR Spectroscopy.** The <sup>31</sup>P NMR spectrum for  $W_2(\mu-H)(\mu-O_2CC_6H_5)Br_4(\mu-dppm)_2 \cdot 2THF$  contained a singlet at 2.7 ppm with  $J_{W-P}$  coupling of 129 Hz. The <sup>1</sup>H spectrum, containing a pentet at 12.8 ppm with  $J_{P-H}$  coupling of 3.7 Hz, and  $J_{W-H}$  coupling of 101 Hz, confirmed the presence of the bridging hydride not observed directly in the solid state. The pentet is shifted only slightly relative to that observed for the chloride analog,  $W_2(\mu-H)(\mu-O_2CC_6H_5)Cl_4(\mu-dppm)_2$  (12.9 ppm).<sup>9</sup> The  $J_{W-H}$  values for both of these hydrides are within the range of coupling values for similar compounds such as  $W_4(\mu-H)_2(O-i-Pr)_{14}$ ,<sup>37</sup> 7.87 ppm, and  $W_2(H)(I)(OCH_2-t-Bu)_6(H_2NMe)_3$ ,<sup>38</sup> 9.2 ppm, with  $J_{W-H}$  values of 95 and 96 Hz, respectively.

The <sup>31</sup>P NMR spectrum for  $W_2(\mu-O_2CC_6H_5)_2I_2(\mu-dppm)_2 \cdot$  solvent displayed a singlet at 39.2 ppm with  $J_{W-P}$  coupling of 117 Hz. While  $W_2(\mu-O_2CC_6H_5)_2I_2(\mu-dppm)_2 \cdot$  solvent is extremely sensitive to moisture and air, the <sup>31</sup>P NMR spectrum of the reaction mixture indicated only the presence of a small

(31) Cotton, F. A.; Felthouse, T. *Inorg. Chem.* **1981**, *20*, 3880.

(32) Fryzuk, M. D.; Kreiter, C. G.; Sheldrick, W. S. *Chem. Ber.* **1989**, *122*, 851.

(33) Chisholm, M. H.; Clark, D. L.; Huffman, J. C.; Van Der Sluys, W. G. *J. Am. Chem. Soc.* **1987**, *109*, 6817.

(34) Chisholm, M. H.; Clark, D. L.; Huffman, J.; Van Der Sluys, W. G.; Kober, E. M.; Lichtenberger, D. L.; Bursten, B. E. *J. Am. Chem. Soc.* **1987**, *109*, 6796.

(35) Franolic, J. D.; Long, J. R.; Holm, R. H. *J. Am. Chem. Soc.* **1995**, *117*, 8139.

(36) Abbott, E. H.; Bose, K. S.; Cotton, F. A.; Hall, W. T.; Sekutowski, J. C. *Inorg. Chem.* **1978**, *17*, 3240.

(37) Akiyama, M.; Chisholm, M. H.; Cotton, F. A.; Extine, M. W.; Haitko, D. A.; Leonelli, J.; Little, D. *J. Am. Chem. Soc.* **1981**, *103*, 779.

(38) Chisholm, M. H.; Huffman, J. C.; Smith, C. A. *J. Am. Chem. Soc.* **1986**, *108*, 222.

amount of one other possible product with a  $^{31}\text{P}$  chemical shift of approximately 16 ppm. This chemical shift occurs in the range expected for  $\text{W}_2\text{I}_4(\mu\text{-dppm})_2$  based on the chemical shifts of  $\text{W}_2\text{Cl}_4(\mu\text{-dppm})_2$  (18.15 ppm) and  $\text{W}_2\text{Br}_4(\mu\text{-dppm})_2$  (15.83 ppm), but this compound represents only a minor product in the reaction.<sup>8</sup> The  $^{31}\text{P}$  NMR spectrum of the reaction mixture in the synthesis of both **3** and **4** did not contain any secondary products. The chemical shifts for the analogous chloride (38.4 ppm) and bromide (38.7 ppm) compounds show slight increases in the chemical shift on progression through the series from Cl to I. This trend is the exact opposite of that observed in complexes with the general formula  $\text{W}_2(\mu\text{-H})(\mu\text{-O}_2\text{CC}_6\text{H}_5)\text{X}_4(\mu\text{-dppm})_2$ ,  $\text{W}_2\text{X}_4(\mu\text{-dppm})_2$  (X is Cl or Br) and  $\text{Mo}_2\text{X}_4(\mu\text{-dppm})_2$  (X is Cl, Br, or I) where a decrease in the chemical shift is observed as one progresses from Cl to less electronegative halides.<sup>8</sup> However, only a 1 ppm chemical shift difference is observed within the halide series, an indication that the phosphorus environments are nearly identical in all of the  $\text{W}_2(\mu\text{-O}_2\text{CC}_6\text{H}_5)_2\text{X}_2(\mu\text{-dppm})_2$  (X = Cl, Br, or I) complexes.

Chemical shift differences of almost 60 ppm from that of free phosphine are observed for **2**, **3**, and **4**, approximately a 20 ppm shift from that of the complex  $\text{W}_2\text{Cl}_4(\mu\text{-dppm})_2$ .<sup>8</sup> While at first the chemical shift difference appears extreme,  $\text{W}_2\text{Cl}_4(\mu\text{-dppe})_2$  has a chemical shift over 50 ppm from that of free dppe. A similar trend though smaller in magnitude is observed for  $[\text{Mo}_2(\mu\text{-O}_2\text{CCH}_3)_2(\mu\text{-dppm})_2][\text{BF}_4]_2$  (19.39 ppm) with a change of 3 ppm from  $\text{Mo}_2\text{Cl}_4(\mu\text{-dppm})_2$ .<sup>8,39</sup> Since  $\text{W}_2\text{Cl}_4(\mu\text{-dppm})_2$  (18.15 ppm) and  $\text{Mo}_2\text{Cl}_4(\mu\text{-dppm})_2$  (16.04 ppm) have very similar chemical shifts, the large chemical shift difference between  $\text{W}_2(\mu\text{-O}_2\text{CC}_6\text{H}_5)_2\text{X}_2(\mu\text{-dppm})_2$  (X is Cl, Br, and I) and  $\text{W}_2\text{Cl}_4(\mu\text{-dppm})_2$  is due to either the presence of the benzoate ligands or the nature of the tungsten halide bonding.<sup>8</sup>

**Diamagnetic Anisotropy of the W–W Bond.** Diamagnetic anisotropy is observed in transition metal complexes due to an induced field from electrons in the multiple bond. In  $\text{W}_2(\mu\text{-O}_2\text{CC}_6\text{H}_5)_2\text{I}_2(\mu\text{-dppm})_2\cdot\text{solvent}$ , the protons of the  $\text{CH}_2$  group in the dppm ligand are affected by the induced field caused by the circulating electrons of the W–W multiple bond. The effect

of this induced field on the chemical shift of the protons in the methylene group of dppm is deshielding resulting in a downfield chemical shift. From the chemical shift difference and positions of these protons calculated from the crystallographic data, the diamagnetic anisotropy for the W–W quadruple bond can be computed from eq 2. In eq 2,  $\Delta\delta$  is the change in the chemical

$$\Delta\delta = \frac{\Delta\chi}{4\pi} \left[ \frac{1 - 3 \cos^2 \theta}{3r^3} \right] = \frac{\Delta\chi}{4\pi} G \quad (2)$$

shift of the proton relative to that in the free ligand,  $r$  is the distance of the proton nucleus from the center of the W–W bond and  $\theta$  is the angle between the  $r$  vector and the center of the W–W axis.<sup>40</sup> Estimates of  $\Delta\chi$  made using this method contain ambiguities concerning the change in the chemical shift ( $\Delta\delta$ ) actually due to  $\Delta\chi$  and change in chemical shift due to ring current effects from the phenyl rings on the ligands. The  $\Delta\chi$  value calculated based on crystallographic and  $^1\text{H}$  spectroscopic data for  $\text{W}_2(\mu\text{-O}_2\text{CC}_6\text{H}_5)_2\text{I}_2(\mu\text{-dppm})_2\cdot\text{solvent}$  is  $-5091 \times 10^{-36} \text{ m}^3 \text{ molecule}^{-1}$ . This value of diamagnetic anisotropy for  $\text{W}_2(\mu\text{-O}_2\text{CC}_6\text{H}_5)_2\text{I}_2(\mu\text{-dppm})_2\cdot\text{solvent}$  is 6–10% lower than values calculated for the W–W bonds found in the complexes of  $\text{W}_2\text{Cl}_4(\mu\text{-dppm})_2$  and  $\text{W}_2\text{Br}_4(\mu\text{-dppm})_2$  which are  $-5596 \times 10^{-36} \text{ m}^3 \text{ molecule}^{-1}$  and  $-5372 \times 10^{-36} \text{ m}^3 \text{ molecule}^{-1}$  respectively.<sup>8</sup>

**Acknowledgment.** K.C.-D. and J.L.E. would like to acknowledge the support of the National Science Foundation EPSCoR program [Grant No. EHR 9108767], ARI Program [Grant No. CHE92-14521]. E.V. and J.Z. acknowledge the support of the Office of Naval Research.

**Supporting Information Available:** Complete tables of crystal data, positional and isotropic equivalent thermal parameters, anisotropic thermal parameters, bond distances, and bond angles for the molecules of  $\text{W}_2(\mu\text{-H})(\mu\text{-O}_2\text{CC}_6\text{H}_5)\text{Br}_4(\mu\text{-dppm})_2\cdot 2\text{THF}$  and  $\text{W}_2(\mu\text{-O}_2\text{CC}_6\text{H}_5)_2\text{I}_2(\mu\text{-dppm})_2\cdot\text{solvent}$  (17 pages). Ordering information is given on any current masthead page. The above and a listing of observed and calculated structure factors (27 pages) are available from author J.L.E. upon request.

IC951617Y

(39) Cotton, F. A.; Eglin, J. L.; Wiesinger, K. J. *Inorg. Chim. Acta* **1992**, *195*, 11.

(40) Cotton, F. A.; James, C. A. *Inorg. Chem.* **1992**, *31*, 5298.